Finite element analysis of three-point bending of a T-beam structural biaxial highly oriented polymer material*)

Ching-Long Wei[1), 2)], Ho Chang[1), **)], Yi-Chang Lee[1)], Rahnfong Lee[1)], Ting-Wei Luo[1)], Jung-Hsuan Chen[3)]

DOI: dx.doi.org/10.14314/polimery.2018.3.6

Abstract: Polymers with biaxial aligned molecular chains are also orthotropic materials, which are characterized by high tensile strength and low shear strength in the length direction. When orthotropic materials are used as structural shapes with poor shear strength, they are likely to undergo premature failure under shear stress. Therefore, in three-point bending, the cross-section of the entire profile not only bears tensile stress and compressive stress in the length direction, but also simultaneously exhibits shear stress. This study analyzes the distribution of tensile stress, compressive stress and shear stress in the length direction of highly oriented polymers (HOP) by finite element analysis to find the most suitable length--to-height ratio for these materials when used as structural shapes. The finite element analysis software, Abaqus, is utilized to simulate HOP T-beam to analyze the load stress of a T-beam. With a fixed cross–section area, as the length of the material changes, its shear strength also changes. Accordingly, the order of occurrence of tensile failure and shear failure can be investigated. The simulation reveals that when the length-to-height ratio is between 4 : 1 and 20 : 1, a zone of stress in which tensile failure and shear failure occur can be found. This result can be exploited in the design and development of structural beam.

Keywords: solid phase processing, highly oriented polymer (HOP), orthotropic materials, T-beam, three-point bending, finite element.

Analiza metodą elementów skończonych zginania trójpunktowego belki teowej wykonanej z wysoko zorientowanego dwuosiowo materiału polimerowego

Streszczenie: Polimery o dwuosiowo zorientowanych łańcuchach makrocząsteczek są materiałami ortotropowymi, wykazującymi dużą wytrzymałość na rozciąganie oraz niewielką wytrzymałość na ścinanie w kierunku długości. Elementy konstrukcyjne wytworzone z materiału ortotropowego o małej wytrzymałości na ścinanie są podatne na przedwczesne uszkodzenie pod wpływem naprężeń ścinających. Przy zginaniu trójpunktowym w przekroju ich profilu występują zarówno naprężenia rozciągające i ściskające w kierunku podłużnym, jak i naprężenia ścinające. Metodą elementów skończonych analizowano rozkład naprężeń rozciągających, ściskających i ścinających w kierunku podłużnym wysoko zorientowanych polimerów (HOP) w celu określenia optymalnego stosunku długości do wysokości w kształtach konstrukcyjnych. Do symulacji naprężeń obciążeniowych w zginaniu trójpunktowym belki teowej wykorzystano program komputerowy Abaqus. Stwierdzono, że przy stałej powierzchni przekroju poprzecznego belki jej wytrzymałość na ścinanie zmienia się wraz ze zmianą długości. Badano również kolejność występowania uszkodzeń pod wpływem działania sił rozciągających i ścinających. Symulacja wykazała, że przy stosunku długości do wysokości w zakresie od 4 : 1 do 20 : 1 występuje strefa naprężeń, w której mogą się pojawiać uszkodzenia w wyniku rozciągania lub ścinania. Uzyskane wyniki można wykorzystać w projektowaniu i optymalizacji belek konstrukcyjnych.

Słowa kluczowe: proces w fazie stałej, wysoko zorientowany polimer, materiały ortotropowe, belka teowa, zginanie trójpunktowe, elementy skończone.

[1)] National Taipei University of Technology, Graduate Institute of Manufacturing Technology, Taipei 10608, Taiwan.

[2)] Lunghwa University of Science and Technology, Department of Mechanical Engineering, Taoyuan 33306, Taiwan.

[3)] National Taiwan Normal University, Department of Industrial Education, Taipei 10610, Taiwan.

*) Materials contained in this article was presented at 2017 Global Conference on Polymer and Composite Materials (PCM 17), 23–25 May 2017, Guangzhou, Guangdong, China.

**) Author for correspondence; e-mail: f10381@ntut.edu.tw

The solid phase process can be used to make molecular chains in a polymer align in the same direction, making the polymer highly oriented. The alignment of molecular chains in a particular direction increases the stiffness of the material and its toughness in the tensile direction [1]. This method for strengthening a polymer is one of the most effective. Many researchers have investigated the processes by which highly oriented polymer can be formed, including ram extrusion, roll drawing, tensile drawing and die drawing [2–5]. Among them, die drawing processing has the broadest range of applications and provides the best strength, and is therefore the most commonly used.

In a study of the relationship between drawing temperature and tensile strength, Ward *et al.* [6–8] argued that a lower drawing temperature yields a stronger highly oriented polymer (HOP). In 1986, Akira Kaito and Kazuo Nakayama *et al.* [9, 10] used polyformaldehyde (POM sheets) to produce polymers with various tensile ratios in the temperature range 140—157 °C, and found that draw ratio is proportional to tensile strength (Fig. 1).

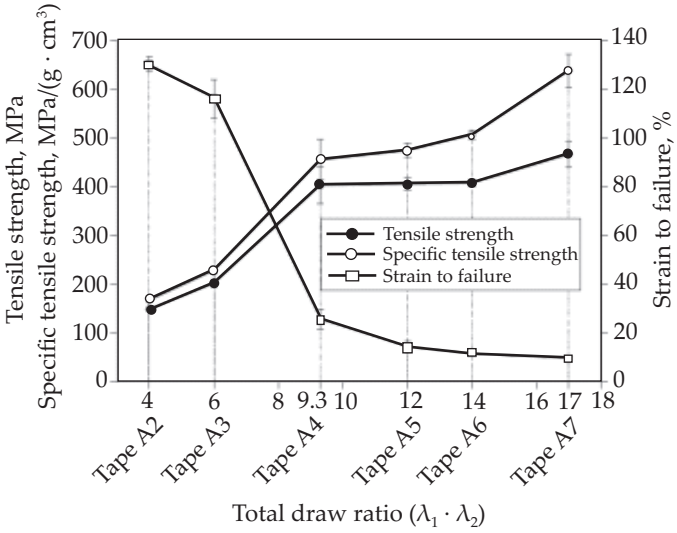

Fig. 1. Draw ratio *versus* tensile strength of die drawing process (according to [10])

In 1996, Taraiya *et al.* [11] used a rotating mandrel assembly and model-type draw forming to produce biaxially oriented polyethylene tubes. Their research revealed that as the axial draw ratio increased with a fixed radial draw ratio, axial tensile strength increased, and radial tensile strength, affected by the increase in axial draw ratio, increased slightly. In 1998, Ellison *et al.* [12] used finite element analysis software, Abaqus, to (elucidate OR analyze) the mechanical behavior of T-beams with various length-to-height ratios. In 2003, Mirza *et al.* [13] used Abaqus to simulate the model-type draw forming process. Their research revealed consistency between simulated and measured draw load, and yielded the optimal process conditions. In 2007, Mohanraj *et al.* [14] used Abaqus to simulate the formation of highly oriented polyoxymethylene rods by model-type draw forming. Both their analytic and their experimental results revealed that model design and important parameters that affect process, such as draw loads and speeds, could be controlled to improve the orientation of highly oriented polyoxymethylene rods and the mechanical properties.

Although the literature discusses tests of mechanical properties, HOP material with different mechanical properties in different directions is extremely different when suffering loading. In three-point bending, a T-beam is typically under tensile stress in the length direction and shear failure commonly occurs. Therefore, in this work, the finite element analysis software, Abaqus, is used to simulate the change in length of HOP with a fixed cross-sectional area, to analyze the position and time of failure, and to obtain the length-to-height ratio at tensile failure.

EXPERIMENTAL PART

In this work, the finite element analysis software, Abaqus, is used to analyze the mechanical behavior of a T-beam under a three-point stress bending load [15]. T-beams are commonly used in engineering and so analysis. The cross-section of the T-beam analyzed in this paper has fixed dimensions (as presented in Fig. 2, which is drawn with reference to the product catalog of the Strongwell Corporation [16]).

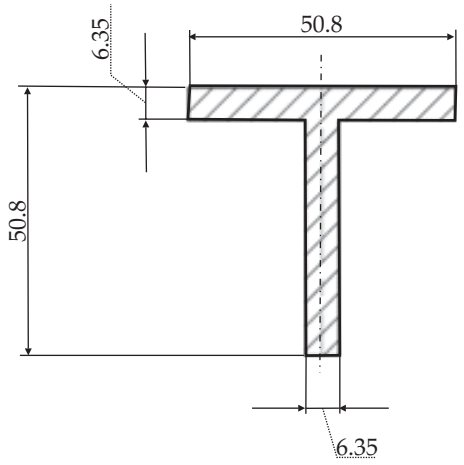

Fig. 2. Dimensions of cross-section of T-beam

The ratios of the lengths of the beam to height considered herein are 4 : 1, 8 : 1, 12 : 1, 16 : 1 and 20 : 1. Both its support and its load are cylinders of equal cross-sectional areas and lengths. Finally, a support beam is placed at each of the two ends of the T-beam, and a load beam is placed halfway along the T-beam's length.

The C3D8I element, which is a three-dimensional eight-node linear hexahedral brick with incompatible modes, is used herein and a downgraded score calculation is carried out to simulate bending moment behavior. C3D8I supports fast calculations easily converge and in this case, yields acceptable. In our case the accuracy is acceptable also. For grid establishment of T-beam, T-beam is firstly divided into four equal parts, and then

their edges are sprayed with nodes every 1.5875 mm. The grids are established after the division. Grids are established for the support beam and the load beam, and the edges thereof are sprayed with nodes to a thickness of 1.5875 mm in all instances. The grids are established after 1.5875 mm division. Figure 3 presents the configuration.

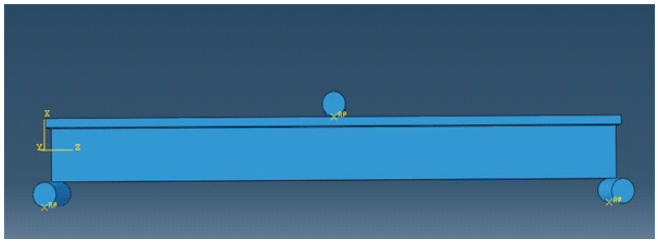

Fig. 3. Configuration of beams

The parameters of the T-beam material are the nine engineering constants of orthotropic materials: E_1, E_2, E_3, Nu_{12}, Nu_{13}, Nu_{23}, G_{12}, G_{13} and G_{23}, which, respectively, correspond to 1-direction module, 2-direction module, 3-direction module, 1–2-direction Poisson's ratio, 1–3-direction Poisson's ratio, 2–3-direction Poisson's ratio, 1–2-direction cutting module, 1–3-direction cutting module, and 2–3-direction cutting module (Table 1).

T a b l e 1. Engineering constants of biaxial HOP

Elastic modulus MPa			Poisson's ratio			Shear modulus MPa		
E_1	E_2	E_3	Nu_{12}	Nu_{13}	Nu_{23}	G_{12}	G_{13}	G_{23}
19 510	5420	20 090	0.07	0.06	0.23	3380	2630	3380

Here, X is direction 1, Y is direction 3, and Z is direction 2. The tensile strength is 482.6 MPa. Table 2 presents the shear strength.

T a b l e 2. Shear strengths of various materials

Material A	Material B	Material C	Material D
55.158 MPa (8000 psi)	75.84 MPa (11 000 psi)	96.53 MPa (14 000 psi)	137.9 MPa (20 000 psi)

Under the constraints on the test beam in the three-point stress bending experiment, a random point on the T-beam both motion (in the X, Y and Z directions) and rotation about the Y-axis have a degree of freedom. Accordingly, any additional load that is generated by fixing the T-beam can be prevented. Contact is made with two supporting cylinders before loading, and the cylinders that apply the load to the T-beam before loading. The supporting beam and the cylinders that apply the load are in contact with the beam. When the load is about to be applied, the two supporting cylindrical beams have no freedom to move in the X, Y, and Z directions or rotate to the three axes. Nevertheless, the cylindrical beams that apply the load to contact surface of beams are displaced in the upward and downward directions, but without displacement or rotation in other directions. Each of the three cylinders is treated as a rigid body.

Static and general analyses, which are useful for understanding engineering issues associated with a three-point bending load, are performed herein. The static and general analysis module in Abaqus/Standard is used. The time increment for computational outputs is 0.01 s.

RESULTS AND DISCUSSION

Position of failures of T-beams with various length-to-height ratios under tensile stress

The results of the computations that were performed using the finite element analysis software, Abaqus, reveal that for all T-beams with length-to-height ratios from 4 : 1 to 20 : 1, tensile failure occurs immediately below the central lower edge (Fig. 4).

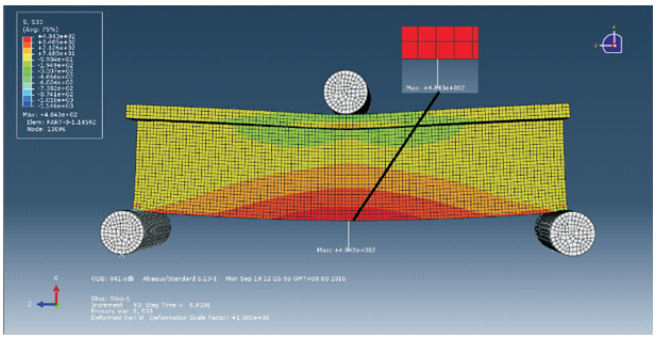

Fig. 4. Position of failure of T-beam with length-to-height ratio of 4 : 1 under tensile stress

Position of failure of T-beams with various length-to-height ratios under shear stress

When shear stress exceeds the shear strength of orthotropic T-beam material, the T-beam undergoes shear failure. Abaqus is used to simulate the shear stress of various materials to locate the shear failures of T-beams with various length-to-height ratios made of various materials. In this work, four materials with different shear strengths (Table 2) – material A, material B, material C and material D – are used. The finite element computational results reveal that except for material D with a length-to-height ratio at 4 : 1, which underwent shear failure at its central lower edge (Fig. 5), all materials exhibited shear failure around the supports at the two ends (Fig. 6).

Order of occurrence of tensile and shear failures in various materials

The results for material A, obtained using Abaqus, include tensile stress, shear stress and time of loading, and displacement. Based on these results, the order of occur-

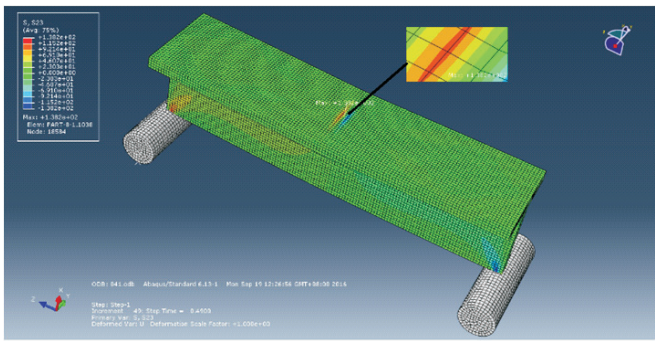

Fig. 5. Position of failure of T-beam with length-to-height ratio of 4 : 1 under shear stress (material D)

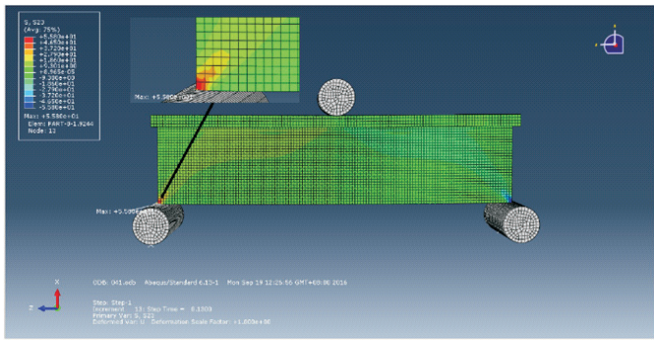

Fig. 6. Position of failure of T-beam with length-to-height ratio of 4 : 1 under shear stress (material A)

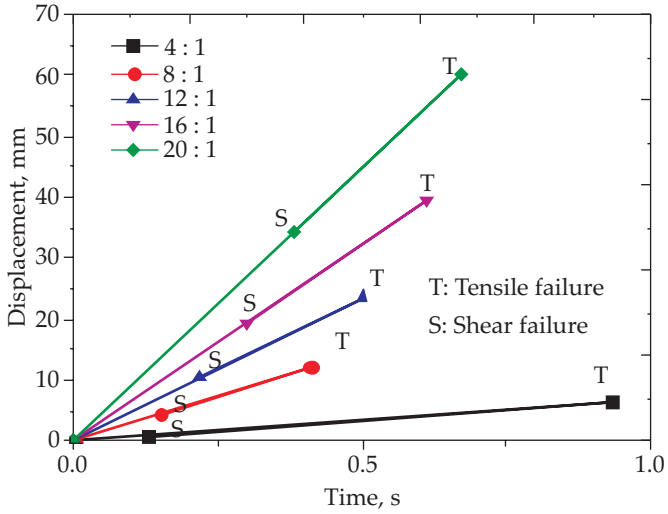

Fig. 7. Order of occurrence of tensile and shear failures for material A

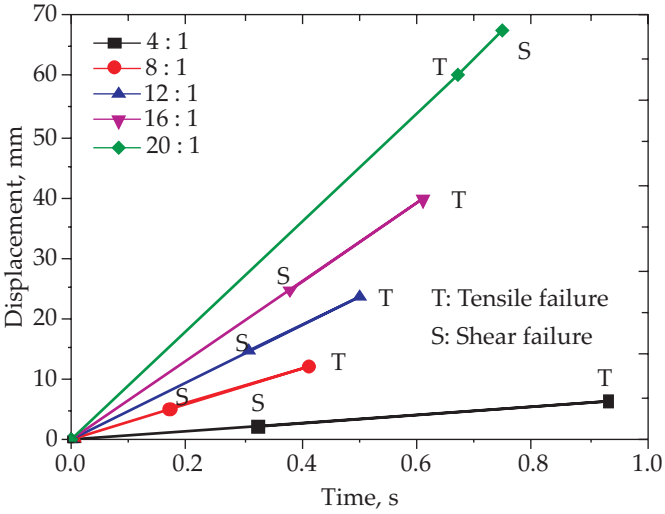

Fig. 8. Order of occurrence of tensile and shear failures for material B

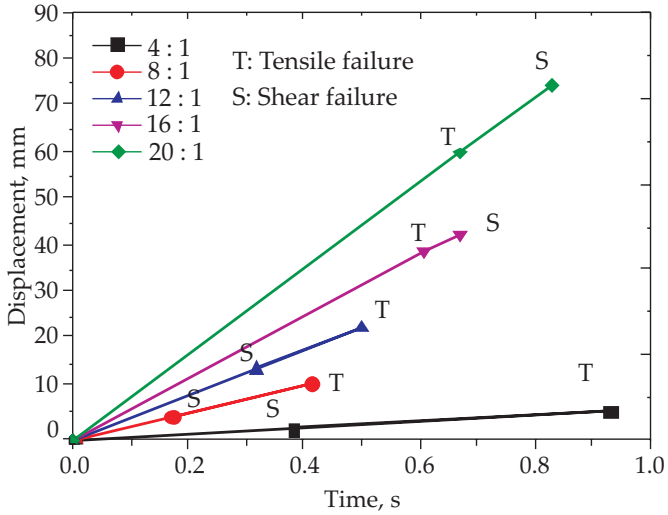

Fig. 9. Order of occurrence of tensile and shear failures for material C

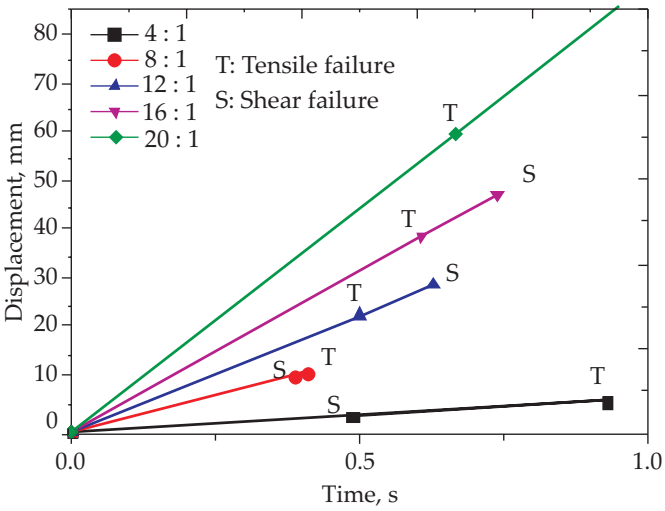

Fig. 10. Order of occurrence of tensile and shear failures for material D

rence of tensile and shear failures of T-beams with various length-to-height ratios is studied (Fig. 7).

As revealed by the computational results for material B, when the length-to-height ratio is between 4 : 1 and 16 : 1 inclusive, shear failure occurs first; when the length-to-height ratio is 20 : 1, tensile failure occurs first (Fig. 8).

The computational results for material C reveal that when the length-to-height ratio is between 4 : 1 and 12 : 1 inclusive, shear failure occurs first; when the length-to-height ratio is 16 : 1 or 20 : 1, tensile failure occurs first (Fig. 9).

According to the computational results for material D, when the length-to-height ratio is 4 : 1 or 8 : 1, shear failure occurs first; when the length-to-height ratio is between

12 : 1 and 20 : 1 inclusive, tensile failure occurs first, and in the case of 20 : 1 shear failure does not occur (Fig. 10).

Through finite element computations, the order of occurrence of the tensile failure and shear failure of T-beams made of orthotropic material is obtained herein. For material A with a shear strength of 55.158 MPa (8000 psi), which is extremely low, at all considered length-to-height ratios of 4 : 1 to 20 : 1, shear failure occurs before tensile failure, so the material cannot be used as a structural material. For material B with a shear strength of 75.84 MPa (11 000 psi) and length-to-height ratios from 4 : 1 to 16 : 1, shear failure occurs first; with a length-to-height ratio of 20 : 1, tensile failure occurs first. Therefore, material B should be used only with a length-to-height ratio of 20 : 1. For material C with a shear strength of 96.53 MPa (14 000 psi) and a length-to-height ratio between 4 : 1 and 12 : 1 inclusive, shear failure occurs first; but when the length-to-height ratio is 16 : 1 or 20 : 1, tensile failure occurs first. Therefore, material C should be used only with a length-to-height ratio of at least 16 : 1. For material D with a shear strength 137.9 MPa (20 000 psi), when the length-to-height ratio is 4 : 1 or 8 : 1, shear failure occurs first, but when it is between 12 : 1 and 20 : 1 inclusive, tensile failure occurs first. Therefore, material D should be used only with length-to-height ratio of at least 12 : 1.

CONCLUSIONS

Even though the tensile strength of orthotropic material is high, the issue of its insufficient poor shear strength must be considered, because tensile failure must precede shear failure for a orthotropic material. The line in Fig. 11 represents the critical value of the shear failure zone and the tensile failure zone of different HOP material.

For materials with various shear strengths, various length-to-height ratios are suggested, and these enable the area of the tensile failure zone of the material to be determined. From the following figure, when orthotropic shear strength is enhanced, tensile failure occurs before shear failure at a lower length-to-height ratio.

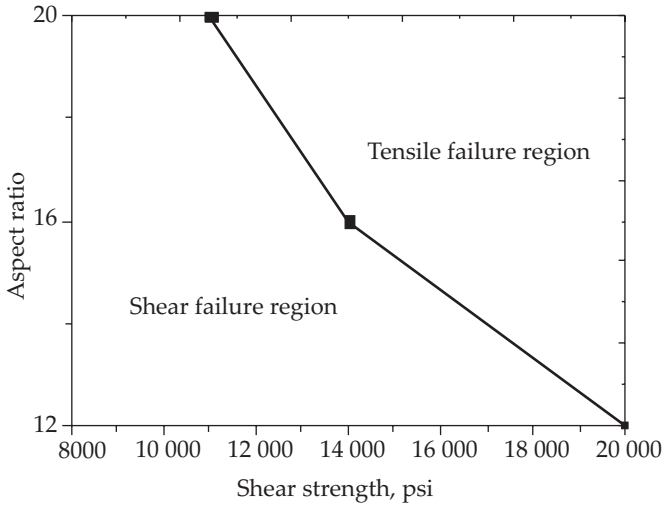

Fig. 11. Shear failure zone and tensile failure zone

REFERENCES

[1] Ward I.M.: *Advances in Polymer Science* **1985**, *70*, 1. http://dx.doi.org/10.1007/3-540-15481-7_6
[2] Coates P.D., Caton-Rose P., Ward I.M., Thompson G.: *Science China Chemistry* **2013**, *56*, 1017. http://dx.doi.org/10.1007/s11426-013-4881-1
[3] Smith P., Lemstra P.J.: *Journal of Materials Science* **1980**, *15*, 505. http://dx.doi.org/10.1007/BF02396802
[4] Rane R.H.: "Microstructure development in solid state processing of polypropylene-talc composites and melt processing of high molecular weight HDPE-clay nanocomposites", Ph.D. Thesis, Michigan State University, Michigan, USA, 2013, p. 2.
[5] Coates P.D., Ward I.M.: *Polymer* **1979**, *20*, 1553. http://dx.doi.org/10.1016/0032-3861(79)90024-7
[6] Theil M.H.: *Journal of Polymer Science Part C: Polymer Letters* **1979**, *17*, 744. http://dx.doi.org/10.1002/pol.1979.130171112
[7] Stehling F.C., Huff T., Speed C.S., Wissler G.: *Journal of Applied Polymer Science* **1981**, *26*, 2693. http://dx.doi.org/10.1002/app.1981.070260818
[8] Richardson A., Hope P.S., Ward I.M.: *Journal of Polymer Science: Polymer Physics Edition* **1983**, *21*, 2525. http://dx.doi.org/10.1002/pol.1983.180211209
[9] Kaito A., Nakayama K., Kanetsuna H.: *Journal of Applied Polymer Science* **1986**, *32*, 3499. http://dx.doi.org/10.1002/app.1986.070320212
[10] Alcock B., Cabrera N.O., Barkoula N.M., Peijs T.: *European Polymer Journal* **2009**, *45*, 2878. http://dx.doi.org/10.1016/j.eurpolymj.2009.06.025
[11] Taraiya A.K., Mirza M.S., Mohanraj J. *et al*.: *Journal of Applied Polymer Science* **2003**, *88*, 1268. http://dx.doi.org/10.1002/app.11848
[12] Ellison M.S., Corona E.: *Journal of Engineering Mechanics* **1998**, *124*, 818. http://dx.doi.org/10.1061/(ASCE)0733-9399(1998)124:8(818)
[13] Mirza M.S., Taraiya A.K., Ward I.M., Barton D.C.: *Proceedings of the Institution of Mechanical Engineers, Part E: Journal of Process Mechanical Engineering* **2003**, *217*, 123. http://dx.doi.org/10.1177/095440890321700203
[14] Mohanraj J., Bonner M.J., Barton D.C., Ward I.M.: *Proceedings of the Institution of Mechanical Engineers, Part E: Journal of Process Mechanical Engineering* **2007**, *221*, 47. http://dx.doi.org/10.1243/0954408JPME95
[15] Abaqus analysis user's manual, Abaqus Inc, 2015, p. 123.
[16] Extren design manual, Strongwell Corp, 1997, p. 38.
[17] Zhao X., Ye L.: *Materials Science and Engineering: A* **2011**, *528*, 4585. http://dx.doi.org/10.1016/j.msea.2011.02.039

Received 20 X 2017.